DOCKETED

Docket Number:	19-IEPR-04
Project Title:	Transportation
TN #:	228787-41
Document Title:	ORNL - Optimal Sizing of a Dynamic Wireless Power Transfer System for Highway Applications
Description:	Oak Ridge National Laboratory (ORNL)
Filer:	Wendell Krell
Organization:	California Energy Commission
Submitter Role:	Commission Staff
Submission Date:	6/19/2019 9:22:42 AM
Docketed Date:	6/19/2019

Optimal Sizing of a Dynamic Wireless Power Transfer System for Highway Applications

A. Foote[1,2], O. C. Onar[2], S. Debnath[2], M. Chinthavali[2], B. Ozpineci[1,2], and D. E. Smith[1,2]
1. The University of Tennessee, Knoxville, TN 37996
2. Power Electronics and Electric Machinery Research Center, Oak Ridge National Laboratory, Knoxville, TN 37932
E-mail: afoote5@vols.utk.edu

***Abstract*- Inductive power transfer has been proposed as a solution to power future automated and electrified highways. In this study, an interoperable wireless charging system is sized so that a light and a heavy-duty vehicle can travel at or near charge-sustaining mode at high speeds using an optimization approach. The conflicting objectives of minimizing the power ratings and the number of inverters, coupler materials, and overall system coverages result in a Pareto Front that is presented in this paper. It is found that a system using short transmitting couplers can ensure high efficiency power transfers to light-duty vehicles (LDVs) and still maintain charge-sustaining operation of heavy-duty vehicles (HDVs). The findings are contextualized by a brief discussion of other aspects relating to the implementation of this technology on roadways such as the impact of the cost of time and travel speeds.**

I. INTRODUCTION

In the future, the large-scale implementation of dynamic wireless power transfer (DWPT) systems in tandem with electric vehicles (EVs) and connected and automated vehicles (CAVs) could revolutionize transportation by enabling faster, charge-sustaining travel with no need to stop for charging. Although most literature currently focuses on low-speed, urban applications for DWPT systems [1], [2], [3], the largest application for the technology may be in long-distance highway travel. There are many ways to justify this: Firstly, the utilization of these roads are higher– in 2014 24% of the total vehicle-miles driven in the U.S. were on the interstate system which is only 1.1% of the road-miles in the nation [4], [5]. This corresponds to the large average annual daily traffic (AADT) volumes and energy-intensive trips seen on highways. Higher system utilization will lower the overall levelized cost of energy (LCOE) as the annual amount of energy provided by the system increases. Secondly, customers will be more motivated to use DWPT charging infrastructure when traveling on highways. Long-distance travel is currently one of the primary contexts of range-anxiety. DWPT will help to resolve this concern by offering a convenient charging solution that can increase the range of CAVs well past that of conventional vehicles. For shorter distances, CAVs may not need to have any range extension during a trip and may instead be charged later or overnight if a lower-cost charging option is available. And finally, some highways and interstates are controlled-access and do not normally have pedestrian cross-traffic. Due to this, lower stray-field mitigation may be needed, and systems can be designed to achieve higher efficiencies.

This manuscript has been authored by the Oak Ridge National Laboratory operated by the UT-Battelle, LLC under Contract No. DE-AC05-00OR22725 with the U.S. Department of Energy.

In DWPT systems, inductive coupling is one of the predominant mechanisms used to transfer power from transmitters in the road to vehicle-side receivers. The transmitters and receivers together form loosely-coupled transformers that use their mutual inductance to transmit power across an airgap as illustrated in Fig. 1. One of the base cases assumes that only one vehicle receiver can couple with each transmitter as the vehicle passes over the transmitter. In this case, the average power the vehicle receives from the roadway is a linear function of the overall percentage of the total roadway with DWPT transmitters, known as coverage, and the average power of a single DWPT system [6]. However, this is a simplistic observation with other details to consider. The achievable power transfer from this DWPT system is also dependent on the area of the receiver and transmitter [7]. For a given airgap, a system with larger couplers on both the road and vehicle sides can usually achieve a higher coupling coefficient and efficiency than a similarly constructed system with smaller couplers. This leads to receiver designs that use most of the area available which, in the application discussed in this paper, may be most of the underside of smaller CAVs.

Regarding the dimensions of the roadside transmitters, a common approach in the literature is to use long tracks much greater in size compared to the receiver dimensions for improved power transfer continuity for increased energy yield. However, this tends to raise the inverter power ratings and voltages. The higher power ratings and voltages are required to accommodate the possible need to efficiently charge multiple vehicles at a time and the higher voltage drops associated with large track self-inductances [8], [9]. Due to these issues, others have focused on lumped element tracks where the transmitter is similar in size to the receiver. This kind of system typically has higher peak efficiencies than track systems but also has its own set of drawbacks. Since lumped-element track designs often use matched coils developed for static charging applications, many of these tracks have rapidly pulsating power outputs and high material costs [10]. To overcome this disadvantage, some works have focused on elongating lumped-element couplers to maintain higher coupling for longer spans to save costs or to

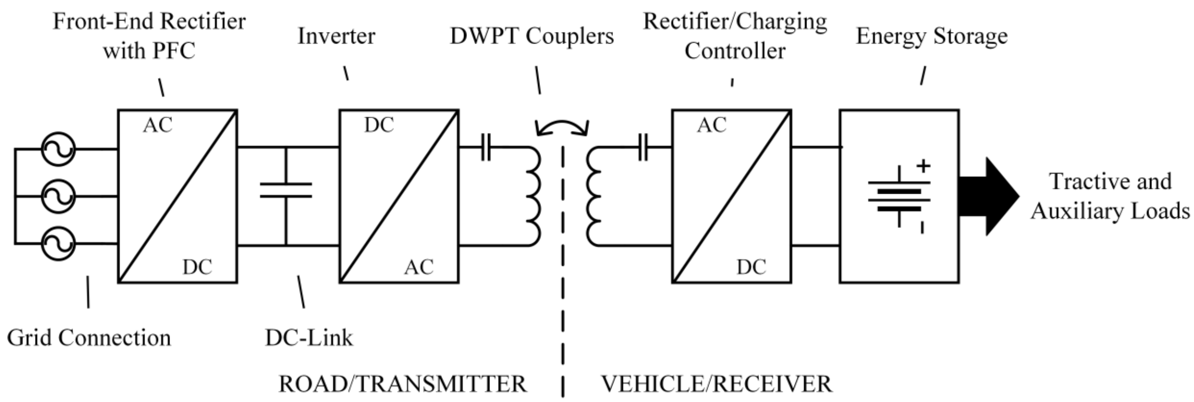

Fig. 1. Simplified overview of a typical DWPT system. Transmitter couplers transfer power through inductive coupling from the road to the vehicle energy storage. This energy is used to power tractive and auxiliary loads.

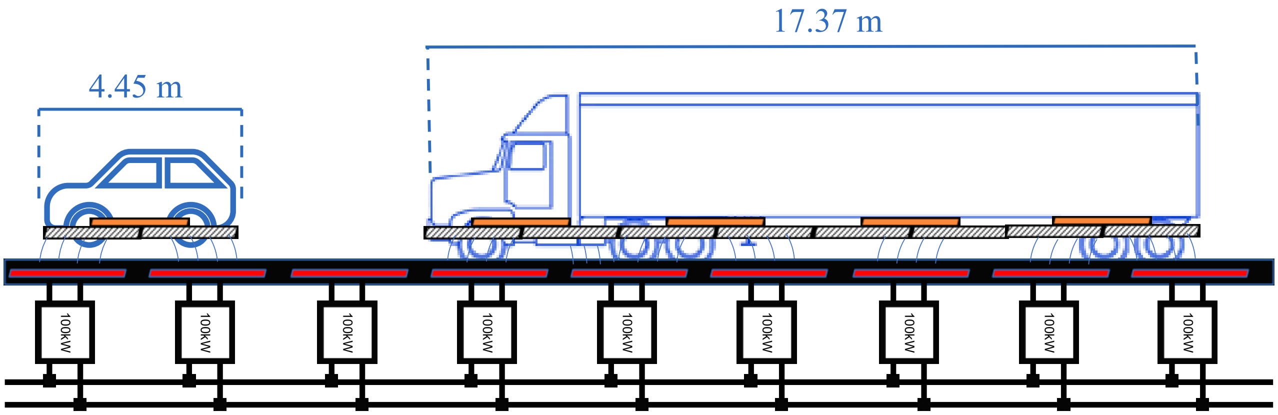

Fig. 2. An example of a DWPT system using paralleled short sectional 100 kW primary couplers and arrays of pickup couplers. As displayed, the light-duty vehicle is receiving 200 kW and the heavy-duty vehicle is receiving 600 kW.

maximize the average efficiency of the system [11], [12].

For a practical highway DWPT system design, the traffic volumes, physical parameters, and power requirements of all classifications of vehicles must be considered. Since the same system may be used to charge all classifications of CAVs [13], it is essential that the DWPT system can operate as efficiently as possible while providing power to each CAV. For example, a DWPT system may be designed to have transmitter lengths shorter than the length of a HDV to maximize efficiency for an LDV. Due to this, it may rely on having multiple receivers on an HDV to scale the power transfer relative to an LDV. A block diagram of such a system with 100 kW transmitters is illustrated in Fig. 2. With 42% roadway coverage, the system could enable charge-sustaining operation for both LDVs and HDVs at 70 mph. Through this example and other examples in literature, the need to consider interoperable operation with many classes of CAVs is clear and further work is needed to practically implement DWPT [2], [14].

In this paper, the power usages of an LDV and a HDV are used to size a DWPT system. The concept of paralleled receivers on HDVs is considered in the design approach to determine the inverter power ratings, DWPT system coverage, and transmitter lengths for charge sustaining mode at constant speed. The approach used here differs from those in the literature [12], [15], [16], [17] by including the transmitter length as a degree of freedom. The system cost components are scaled by appropriate economic values and then multiplied by varying weighting factors to produce the objective function.

II. METHODOLOGY

A. *Vehicle Energy Use*

Vehicle energy use determines the average power required from the DWPT system on the highway. As derived from expressions in [18] and [19], the average tractive power $\bar{P}$ used by CAVs over driving profiles and at a constant speed is provided in (1). Equation (1) includes vehicle mass M, velocity $v(t)$, acceleration $a(t)$, road grade α, and aerodynamic form factor $C_{\mathrm{d}}A$. The constants for rolling friction $\mu_{\mathrm{r}} = 0.0065$, mass correction coefficient $\delta = 1.04$, and air density at standard temperature and pressure ρ were also considered. By splitting up the time periods with positive and negative power, the different efficiencies associated with CAVs positive wheel work and regenerative braking were considered in (1). These efficiencies, η_{eq} and η_{br}, are assumed to be constants [20]. Using (1), the energy need for vehicles on a stretch of highway or interstate can be estimated using average annual daily traffic (AADT) counts, freight weights, and velocity data from microwave radar stations and vehicle trajectory surveys from

$$\bar{P} = \frac{1}{\mathrm{T}}\int_0^T \left(\frac{(\mu_{\mathrm{r}} + \sin(\alpha))Mg}{\eta_{\mathrm{eq}}}v(t) + \frac{C_{\mathrm{d}}Av(t)^3\rho}{2\eta_{\mathrm{eq}}} + \frac{\delta Ma(t)v(t)}{\eta_{\mathrm{eq}}}\right)^{P>0} + \left((\mu_{\mathrm{r}} + \sin(\alpha))Mg\eta_{\mathrm{br}}v(t) + \frac{C_{\mathrm{d}}A\eta_{\mathrm{br}}v(t)^3\rho}{2} + \delta M\eta_{\mathrm{br}}a(t)v(t)\right)^{P<0} dt \qquad (1)$$

TABLE I

PARAMETERS FOR VEHICLE MODELS AND CONSTANT SPEED RESULTS

Light Duty Model		Heavy Duty Model	
Parameter	Value	Parameter	Value
M	1700 kg	M	33021 kg
$C_d A$	0.72 m^2	$C_d A$	7.88 m^2
ℓ_{vehicle}	4.45 m	ℓ_{vehicle}	17.37 m
P_{aux}	3 kW	P_{aux}	6 kW
Power Use at Constant Speed (Not Including Auxiliary Power)			
55 mph	12.93 kW	55 mph	145.26 kW
70 mph	23.39 kW	70 mph	251.41 kW
80 mph	33.04 kW	80 mph	359.12 kW

microwave radar stations and vehicle trajectory surveys from past years. Currently, the total and relative numbers of weight classifications vary widely by time of day [2] and location [4], and the energy usage of each vehicle depend furthermore on individual driving style preferences [19]. Due to these inherent complexities, a constant speed of 70 mph on a flat road is assumed in this paper and the average power is calculated using (1) for a light-duty and heavy-duty vehicle as in Table 1. The physical parameters are based on current electric passenger vehicles and typical on-road weights for Class 8 trucks [5]. Additional loads not used for vehicle propulsion called auxiliary loads have also been included as P_{aux}. For future EVs and CAVs, passenger entertainment, HVAC, onboard computers, communication devices, and sensors may use significant power. The auxiliary power values used here are derived from equivalent HVAC loads at low ambient temperatures [21].

B. DWPT System Efficiency

The impact of overall system efficiency is important for the DWPT system design and must be quantified. The efficiency of inductive couplers, when optimally loaded, can be expressed as (2) [7], [12].

$$\eta = \frac{k^2 Q_T Q_R}{\left(1+\sqrt{1+k^2 Q_T Q_R}\right)^2}. \tag{2}$$

From this, one path to high efficiency is by designing couplers with high quality factors. The quality factors are given as $Q_T=\omega L_T/R_T$ and $Q_R=\omega L_R/R_R$ for the transmitter and receiver respectively. The self-inductances L_T, L_R and resistances R_T, R_R of the transmitter and receiver are used in the definition of quality factors. Overall, the quality factors might be increased by raising the operating frequency of the system and by using well-designed Litz wire conductors and ferrite structures. It can be shown that the quality factor will remain constant with respect to variations in coupler length because resistance and self-inductance will increase at the same rate as length increases [12]. Due to this, the quality factors are set as $Q_T = Q_R = 30$ in this analysis. This value represents a typical a low-cost DWPT system design. The other way to raise efficiency is to increase the mutual inductance between the couplers. As mentioned previously, this can be done first by increasing the receiver area to fill the available space on the underside of an LDV. For a

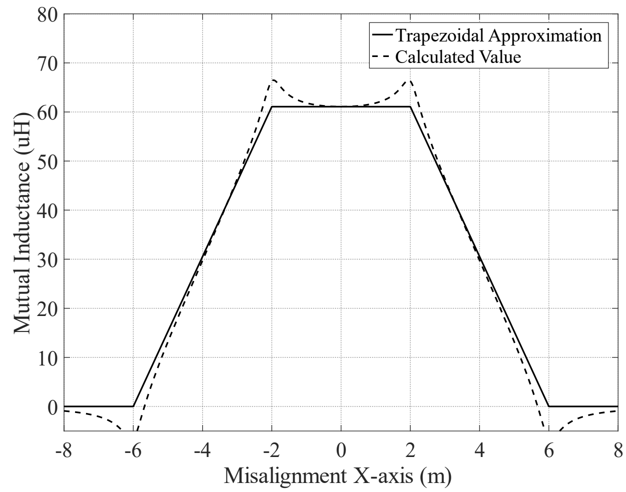

Fig. 3. The mutual inductance of a DWPT system over misalignment in the direction of travel. Here the transmitter dimensions are 8x2 meters, and the receiver dimensions are 4x2 meters. The number of turns of the transmitter and receiver are 4 and 4, respectively, and the airgap is 20 cm.

matched transmitter, this will result in a higher mutual inductance and a higher coupling coefficient, thus yielding higher efficiency by (2). However, once the available receiver area is filled out, the maximum mutual inductance of the inductive link will not increase any further, and the coupling coefficient will decrease as L_T continues to increase. Because of this, there exists a tradeoff between coupler length and efficiency which must be considered in sizing an optimal DWPT system.

The coupling coefficient of the system must be determined over the span of travel-direction misalignments and overhead positions to find the best-case overall efficiency $\eta_{\text{coupler}}(\ell_T)$ of a DWPT system. $\eta_{\text{coupler}}(\ell_T)$ is the average of (2) over the length of the transmitter ℓ_T. The analytical expressions in (3)-(4) [22] and (5) [23] are used in this work to calculate mutual and self-inductance. The mutual inductance expressions in (3) and (4) assume that the multiple turns of the couplers are close to one another and can be modeled as identical filament rectangular coils with vertices ABCD for the transmitter and EFGH for the receiver. The length of the sides of the couplers are measured as $2a$ and $2b$ for the transmitter and $2c$ and $2d$ for the receiver. As in [22], the fluxes within the receiver from each segment of the transmitter in the vertical direction are Φ_{AB-z}, Φ_{BC-z}, Φ_{CD-z}, and Φ_{DA-z}.

$$\Phi_{\mathrm{CD-z}} = \frac{\mu_0}{2\pi}\Bigg[\sqrt{(b+d)^2+z^2+(a+c)^2} - (a+c)\cdot\operatorname{arctanh}\frac{a+c}{\sqrt{(b+d)^2+z^2+(a+c)^2}} - \sqrt{(b+d)^2+z^2+(a-c)^2} + (a-c)\cdot\operatorname{arctanh}\frac{a-c}{\sqrt{(b+d)^2+z^2+(a-c)^2}} - \sqrt{(b-d)^2+z^2+(a+c)^2} - (a+c)\cdot\operatorname{arctanh}\frac{a+c}{\sqrt{(b-d)^2+z^2+(a+c)^2}} + \sqrt{(b-d)^2+z^2+(a-c)^2} - (a-c)\cdot\operatorname{arctanh}\frac{a-c}{\sqrt{(b-d)^2+z^2+(a-c)^2}}\Bigg] \quad (3)$$

$$M = N_{\mathrm{T}}N_{\mathrm{R}}(\Phi_{\mathrm{AB-z}}+\Phi_{\mathrm{BC-z}}+\Phi_{\mathrm{CD-z}}+\Phi_{\mathrm{DA-z}}) \quad (4)$$

$$L_{\mathrm{T}} = \frac{\mu_0}{\pi}N_{\mathrm{T}}^2\Bigg[2a\cdot\ln\frac{8ab}{r_{\mathrm{T}}\cdot\left((2a)+\sqrt{(2a)^2+(2b)^2}\right)} + 2b\cdot\ln\frac{8ab}{r_{\mathrm{T}}\cdot\left((2b)+\sqrt{(2a)^2+(2b)^2}\right)} - 2\cdot\left(2a+2b-\sqrt{(2a)^2+(2b)^2}\right) + 0.25(2a+2b)\Bigg] \quad (5)$$

To determine the mutual inductance over misalignments, a trapezoidal approximation is used as illustrated in Fig. 3 [11]. Though not used here, (3) can also be modified to include misalignment by adding x_{offset} or y_{offset} to every c or d term [24]. Due to dependency of self-inductance to conductor radius in (5), constant conductor radii are assumed for the transmitter r_{T} and receiver r_{R}. A similar expression is used for L_{R}. For this application, the impact of wire-radius on the mutual inductance calculation is minimal because the size of the couplers is large compared to the wire sections [22]. In this work, the length of the receiver ℓ_{R} is set to 4.45 m, the length of the LDV, and the width of the transmitter and receiver are $W_{\mathrm{T}} = W_{\mathrm{R}} = 1$ m, which represent the available width within the axle track of the LDV. The airgap for the system z is set at 20 cm, the ground clearance of the LDV. Furthermore, the number of turns of both couplers are set as $N_{\mathrm{T}} = N_{\mathrm{R}} = 4$.

The use of (3)-(5) inherently limits this analysis to rectangular, air-core couplers for the transmitter and receiver, but similar conclusions about the relationship between coupler lengths and system efficiency have also been reached with a bipolar system with ferrites [12].Other works further justify the use of similar analytical expressions in system optimizations [23], [25]. To expand this methodology to a specific coupler design, it may be necessary to use one of several finite-element tools available to accurately model the inductances of the system [7], [26].

$$\min_{\mathbf{x}} \quad f(\mathbf{x},\mathbf{p}) = \mathrm{W_1W_2C_{inv}}(\mathbf{x},\mathbf{p}) + (1-\mathrm{W_1})\mathrm{W_2}\cdot\mathrm{C_{road}}(\mathbf{x},\mathbf{p}) + (1-\mathrm{W_2})\mathrm{C_{coupler}}(\mathbf{x},\mathbf{p}) \quad (6)$$

$$\bar{P} + P_{\mathrm{aux}} - P_{\mathrm{sys}}\cdot\frac{\ell_{\mathrm{vehicle}}}{\ell_{\mathrm{T}}}\cdot\beta_{\mathrm{road}}\cdot\eta_{\mathrm{coupler}}(\ell_{\mathrm{T}}) \le 0$$
$$[0 \quad 0.5 \quad 0]^T \le [P_{\mathrm{sys}} \quad \ell_{\mathrm{T}} \quad \beta_{\mathrm{road}}]^T \le [500\text{ kW} \quad 10\text{ m} \quad 1]^T \quad (7)$$
$$\mathrm{W_i} \in (0,1)$$

$$\mathrm{C_{inv}}(\mathbf{x},\mathbf{p}) = \frac{P_{\mathrm{sys}}\beta_{\mathrm{road}}}{\ell_{\mathrm{T}}} \quad (8)$$

$$\mathrm{C_{road}}(\mathbf{x},\mathbf{p}) = \beta_{\mathrm{road}} \quad (9)$$

$$\mathrm{C_{coupler}}(\mathbf{x},\mathbf{p}) = \frac{P_{\mathrm{sys}}\beta_{\mathrm{road}}}{\ell_{\mathrm{T}}}\cdot(2\ell_{\mathrm{T}}+2W_{\mathrm{T}})\cdot N_{\mathrm{T}} \quad (10)$$

C. Multi-Objective Optimization

Based on the models developed, a multi-objective function can be written, as shown in (6)-(10), to minimize capital costs. The upper bound chosen for the system power rating P_{sys} is based on the limits of the current state-of-art high-power wireless power transfer systems [27]. Three objective functions are used: $\mathrm{C_{inv}}(\mathbf{x},\mathbf{p})$ represents the cost of power electronics, $\mathrm{C_{road}}(\mathbf{x},\mathbf{p})$ is the cost of road construction, and $\mathrm{C_{coupler}}(\mathbf{x},\mathbf{p})$ approximates the cost of the coupler material. The system variables $\mathbf{x}$ are the system power rating P_{sys}, transmitter length ℓ_{T}, and coverage β_{road}. Other parameters of the system and vehicles $\mathbf{p}$ are ℓ_{vehicle}, $\bar{P}$, P_{aux}, and W_{T}. The constraints of the optimization in (7) are charge-sustaining operation for the light and heavy-duty vehicles at a constant speed of 70 mph.

There are several assumptions inherent to this formulation. $\mathrm{C_{inv}}(\mathbf{x},\mathbf{p})$ is calculated by considering the number of power electronic converters needed when each inverter is connected to one transmitter. $\mathrm{C_{road}}(\mathbf{x},\mathbf{p})$ is modeled as the road construction costs for trenching and resurfacing roadways to install the system. $\mathrm{C_{coupler}}(\mathbf{x},\mathbf{p})$ is calculated as proportional to the amount of wire in air-core transmitters, given that the needed section of Litz wire is proportional to P_{sys} for a fixed output voltage. All these functions are scaled by appropriate economic values and then multiplied by varying weighting factors W_{i} to produce the objective function. This, with the inclusion of $\eta_{\mathrm{coupler}}(\ell_{\mathrm{T}})$ in the constraints is used to generate the Pareto fronts of solutions as seen in the following section by using a weighted sum method [28].

III. RESULTS

As seen from the results in Fig. 4, it is important to limit the coverage of DWPT systems due to the large expense of roadway construction. However, there are practical tradeoffs between the power rating and coverage of the system. With low coverages, the onboard energy storage and electronics of EVs must facilitate high charge rates. However, the power ratings in this case may still be lower than what would be required with high-

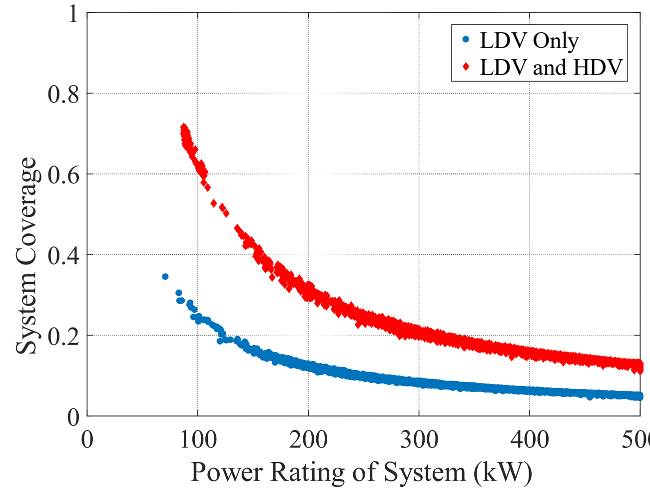

Fig. 4. Pareto solutions from (6)-(10) for two different cases: one with the LDV only at 70 mph and the other with both the LDV and HDV at 70 mph. The system length axis is excluded as all solutions are around 4.45 m.

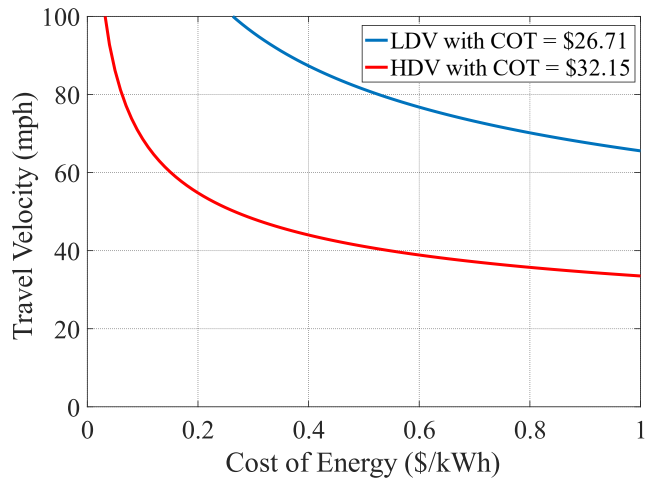

Fig. 5. Optimal travel speeds for LDV and HDV considering example costs of time (COT) and costs of energy. If low-cost energy is available, travel speeds may rise in the future if appropriate CAVs and roads are available.

power static charging because the DWPT system can transfer energy over a longer period of time than static charging systems while the EV is on the move. There is also an upper limit to the area-related power density that can be achieved by wireless-charging systems (not considered here).

The density of solutions around $\ell_T = 4.45$ m in Fig. 4 demonstrates that the length of the transmitters plays a critical role in determining the optimal DWPT system because it is a main variable in the overall efficiency of the system. This sensitivity to length increases with low quality factors. Due to this, scaling power levels for HDVs by utilizing their longer lengths to include multiple receivers is a design feature that may prove essential to allow more types of vehicles to use the same infrastructure. Different placement schemes could also be considered. Though not proven here, the close-packed, adjacent transmitter spacing illustrated in Fig. 2 could also be spread over a greater distance without impacting the average charging level. One important motivation of doing this is reducing maximum charge rates while maintaining the same average energy transfer as the adjacent spacing case displayed in Fig. 2.

IV. Discussion

The analysis within this study focuses on the design of a DWPT system from a minimizing capital cost perspective. From this viewpoint alone, efficiency is already shown to be important in the selection of the system parameters. However, the effect on the operating costs of the DWPT system must also be considered. For a low efficiency system, there will be a large amount of wasted energy which will introduce additional costs over the lifetime of the system.

Another aspect to operating cost is travel time [17]. Several numbers are available to help quantify this effect: for instance, in January 2018, the average wage was $26.71 per hour [29] and similarly the average cost of freight delay has been determined to be $32.15 per hour [30] in the USA. With these and other values, different case studies can be performed for each stretch of highway or interstate to analyze the impact of slowing down to receive more charging energy. For example, in the future, individuals or freight with a high associated cost of time travelling in CAVs may choose to pay more for energy to reach their destinations faster by increasing travel speed. For a given charging scheme, energy cost, and vehicle type, an optimal travel speed can be calculated with time modeled as an equivalent cost. As an example, the two vehicle models in Table 1 are used with (1) to find the optimal constant trip velocity for different combinations of costs of energy and costs of time (COT) as shown in Fig. 5. It is assumed that there are no charging limitations, stops, or speed restrictions. This simple example illustrates the importance of providing low-cost charging solutions for long-distance travel.

The effect of slowing down over DWPT system can be modeled similarly. If vehicles slow down over DWPT systems, a lower-powered system with lower coverages could be used. However, the reduction in capital costs from this may also be offset to some extent by the increased travel time spent by CAVs on the roadway. In fact, for large volumes of traffic, the equivalent cost of slowing down may outweigh the reduction in capital costs and justify making the system charge-sustaining at full speed. With these and other considerations, similar case studies can be done to compare DWPT to static charging systems. System-level studies such as these will provide insight into the final practical use of DWPT and help speed the pace of adoption of DWPT technologies on roadways.

V. Conclusion

Sizing and designing a full-scale DWPT system for highway applications is a vast problem area that has not been fully addressed in the literature. As shown by this analysis, the system parameters must be selected carefully to reduce the overall cost per mile of DWPT. Among these features, system length is important due to its impact on the system coupling coefficient and overall efficiency. The impact of this effect will increase if the quality factor of the system is low. Because high-efficiency operation is paramount for DWPT to be practical from both a capital and operational cost standpoint and the quality factors of systems may be limited, transmitter sizes will be constrained by the dimensions of smaller vehicles. In this case, it is advantageous to consider utilizing the longer lengths of heavier vehicles to have multiple paralleled receivers. This will both decrease the initial capital cost and ensure the maximum utilization of the DWPT system which will drive down the cost of using the system for all. If these costs are low enough, DWPT could revolutionize future transportation by eliminating range-anxiety and enabling long distance, charge-sustaining trips in CAVs. This would increase the mobility of both freight and passengers and ultimately help remove the barrier of long-distance travel from transportation electrification.

ACKNOWLEDGMENTS

This paper and the work described were sponsored by the U.S. Department of Energy (DOE) Vehicle Technologies Office (VTO) under the Systems and Modeling for Accelerated Research in Transportation (SMART) Mobility Laboratory Consortium, an initiative of the Energy Efficient Mobility Systems (EEMS) Program. The authors acknowledge Mr. John Smart of the Idaho National Laboratory for leading the Advanced Fueling Infrastructure Pillar of the SMART Mobility Laboratory Consortium. Authors also would like to thank Mr. David Anderson who leads the DOE VTO Energy Efficient Mobility Systems program for establishing the project concept, advancing implementation, and providing ongoing guidance.

The authors would also like to thank Mr. Jared Baxter for his review and input over the course of this work.

REFERENCES

[1] S. Chopra and P. Bauer, "Driving Range Extension of EV With On-Road Contactless Power Transfer - A Case Study," *IEEE Transactions on Industrial Electronics,* vol. 60, no. 1, pp. 329-338, 2013.

[2] Transport Research Laboratory, "Feasibility Study: Powering Electric Vehicles on England's Major Roadways," Highways England 2015, Available: http://assets.highways.gov.uk/specialist-information/knowledge-compendium/2014-2015/Feasibility+study+Powering+electric+vehicles+on+Englands+major+roads.pdf.

[3] Z. Pantic, S. Bai, and S. M. Lukic, "Inductively coupled power transfer for continuously powered electric vehicles," in *2009 IEEE Vehicle Power and Propulsion Conference*, 2009, pp. 1271-1278.

[4] "Highway Statistics 2014," Federal Highway Administration, Washington, DC USA 2014, Available: https://www.fhwa.dot.gov/policyinformation/statistics/2014/.

[5] Oak Ridge National Laboratory. (2017). *Transportation Energy Data Book*. Available: http://cta.ornl.gov/data/index.shtml

[6] A. Foote, B. Ozpineci, M. Chinthavali, and J. M. Li, "Sizing Dynamic Wireless Charging for Light-Duty Electric Vehicles in Roadway Applications," *IEEE PELS Workshop on Emerging Technologies: Wireless Power (2016 Wow),* pp. 224-230, 2016.

[7] R. Bosshard, J. W. Kolar, J. Muhlethaler, I. Stevanovic, B. Wunsch, and F. Canales, "Modeling and η - α -Pareto Optimization of Inductive Power Transfer Coils for Electric Vehicles," *IEEE Journal of Emerging and Selected Topics in Power Electronics,* vol. 3, no. 1, pp. 50-64, 2015.

[8] C. C. Mi, G. Buja, S. Y. Choi, and C. T. Rim, "Modern Advances in Wireless Power Transfer Systems for Roadway Powered Electric Vehicles," *IEEE Transactions on Industrial Electronics,* vol. 63, no. 10, pp. 6533-6545, Oct 2016.

[9] J. H. Kim *et al.*, "Development of 1-MW Inductive Power Transfer System for a High-Speed Train," *IEEE Transactions on Industrial Electronics,* vol. 62, no. 10, pp. 6242-6250, 2015.

[10] G. Buja, M. Bertoluzzo, and H. K. Dashora, "Lumped Track Layout Design for Dynamic Wireless Charging of Electric Vehicles," *IEEE Transactions on Industrial Electronics,* vol. 63, no. 10, pp. 6631-6640, Oct 2016.

[11] M. Bertoluzzo, G. Buja, and H. K. Dashora, "Design of DWC System Track with Unequal DD Coil Set," *IEEE Transactions on Transportation Electrification,* vol. 3, no. 2, pp. 380-391, 2017.

[12] Z. Wei, W. Siu-Chung, C. K. Tse, and C. Qianhong, "An Optimized Track Length in Roadway Inductive Power Transfer Systems," *IEEE Journal of Emerging and Selected Topics in Power Electronics,* vol. 2, no. 3, pp. 598-608, 2014.

[13] P. Fyhr, G. Domingues, M. Andersson, F. J. Márquez-Fernández, H. Bängtsson, and M. Alaküla, "Electric roads: Reducing the societal cost of automotive electrification," in *2017 IEEE Transportation Electrification Conference and Expo (ITEC)*, 2017, pp. 773-778.

[14] B. J. Limb, B. Crabb, R. Zane, T. H. Bradley, and J. C. Quinn, "Economic Feasibility and Infrastructure Optimization of In-Motion Charging of Electric Vehicles Using Wireless Power Transfer," *IEEE Pels Workshop on Emerging Technologies: Wireless Power (2016 Wow),* pp. 42-46, 2016.

[15] B. J. Limb, "Optimization of Roadway Electrification Integrating Wireless Power Transfer: TechnoEconomic Assessment and Lifecycle Analysis," Ph.D. Thesis, Utah State University, 2017.

[16] S. Jeong, Y. J. Jang, and D. Kum, "Economic Analysis of the Dynamic Charging Electric Vehicle," *IEEE Transactions on Power Electronics,* vol. 30, no. 11, pp. 6368-6377, 2015.

[17] M. D. Fuller, "Wireless Charging in California: Range, Recharge, and Vehicle Electrification," 3646289 Ph.D. Thesis, University of California, Davis, 2014.

[18] L. Guzzella and A. Sciarretta, *Vehicle Propulsion Systems*. 2013.

[19] I. M. Berry, "The effects of driving style and vehicle performance on the real-world fuel consumption of US light-duty vehicles," Thesis, Massachusetts Institute of Technology, 2010.

[20] Argonne National Laboratory (ANL). *Downloadable Dynamometer Database (D3)*. Available: https://www.anl.gov/energy-systems/group/downloadable-dynamometer-database

[21] H. C. Frey, P.-Y. Kuo, and C. Villa, "Effects of Idle Reduction Technologies on Real World Fuel Use and Exhaust Emissions of Idling Long-Haul Trucks," *Environmental Science & Technology,* vol. 43, no. 17, pp. 6875-6881, 2009.

[22] Y. Cheng and Y. Shu, "A New Analytical Calculation of the Mutual Inductance of the Coaxial Spiral Rectangular Coils," *IEEE Transactions on Magnetics,* vol. 50, no. 4, pp. 1-6, 2014.

[23] J. Sallan, J. L. Villa, A. Llombart, and J. F. Sanz, "Optimal Design of ICPT Systems Applied to Electric Vehicle Battery Charge," *IEEE Transactions on Industrial Electronics,* vol. 56, no. 6, pp. 2140-2149, Jun 2009.

[24] A. Poorfakhraei, G. Movaghar, and F. Tahami, "Optimum design of coils in a dynamic wireless electric vehicle charger with misalignment compensation capability," in *2017 8th Power Electronics, Drive Systems & Technologies Conference (PEDSTC)*, 2017, pp. 419-424.

[25] X. Zhang, Z. Y. Yuan, Q. X. Yang, Y. J. Li, J. G. Zhu, and Y. Li, "Coil Design and Efficiency Analysis for Dynamic Wireless Charging System for Electric Vehicles," *IEEE Transactions on Magnetics,* vol. 52, no. 7, Jul 2016.

[26] M. Moghaddami, A. Anzalchi, and A. I. Sarwat, "Finite element based design optimization of magnetic structures for roadway inductive power transfer systems," in *2016 IEEE Transportation Electrification Conference and Expo (ITEC)*, 2016, pp. 1-6.

[27] A. Foote and O. C. Onar, "A review of high-power wireless power transfer," in *2017 IEEE Transportation Electrification Conference and Expo (ITEC)*, 2017, pp. 234-240.

[28] I. Y. Kim and O. L. de Weck, "Adaptive weighted sum method for multiobjective optimization: a new method for Pareto front generation," *Structural and Multidisciplinary Optimization,* vol. 31, no. 2, pp. 105-116, 2005.

[29] US Bureau of Labor Statistics. Total Private Average Hourly Earnings of All Employees [Online]. Available: https://www.bls.gov/data/

[30] US Federal Highway Administration, "An Initial Assessment of Freight Bottlenecks on Highways," 2005, Available: https://www.fhwa.dot.gov/policy/otps/bottlenecks/index.cfm.